COMPDYN 2019
7th ECCOMAS Thematic Conference on
Computational Methods in Structural Dynamics and Earthquake Engineering
M. Papadrakakis, M. Fragiadakis (eds.)
Crete, Greece, 24–26 June 2019

RINTC-E: TOWARDS SEISMIC RISK ASSESSMENT OF EXISTING RESIDENTIAL REINFORCED CONCRETE BUILDINGS IN ITALY

Paolo Ricci[1,*], Vincenzo Manfredi[2], Fabrizio Noto[3], Marco Terrenzi[4], Maria Teresa De Risi[1], Mariano Di Domenico[1], Guido Camata[4], Paolo Franchin[3], Angelo Masi[2], Fabrizio Mollaioli[3], Enrico Spacone[4], and Gerardo M. Verderame[1]

[1] Department of Structures for Engineering and Architecture, University of Naples Federico II
Via Claudio, 21 - 80125 Naples - Italy
{paolo.ricci,mariateresa.derisi,mariano.didomenico,verderam}@unina.it

[2] University of Basilicata, School of Engineering
85100 Potenza - Italy
enzo.manfredi@alice.it, angelo.masi@unibas.it

[3] Sapienza University of Rome, Department of Structural and Geotechnical Engineering
Via Gramsci 53 - 00197 Rome - Italy
fabrizio.noto@gmail.com, paolo.franchin@uniroma1.it, fabrizio.mollaioli@uniroma1.it

[4] University G. d'Annunzio of Chieti-Pescara, Department of Engineering and Geology
Viale Pindaro 42 - 65127 Pescara - Italy
{marco.terrenzi,guido.camata,espacone}@unich.it

Abstract

The RINTC research project (RINTC Workgroup, 2018), financed by the Italian Department of Civil Protection, is aimed at evaluating the seismic risk of buildings conforming to the Italian building code. Within the framework of this project, the attention has been recently focused on existing buildings, too. In this study, case-study structures, representative of the existing residential reinforced concrete (RC) building stock in Italy, are analyzed. These structures are three-storey buildings with compact rectangular plan, and they have been defined through a simulated design process, in order to represent two types of buildings, namely designed for gravity loads only during 1970s (gravity load designed, GLD) or for moderate seismic loads during 1990s (seismic load designed, SLD). GLD buildings are assumed to be located in three different sites, namely Milan, Naples and Catania, in increasing order of seismic hazard. SLD buildings are assumed to be located in L'Aquila. The assumed design typologies are consistent with the seismic classification of the sites at the assumed ages of construction. The presence of typical nonstructural masonry infill walls (uniformly distributed in plan as external enclosure walls) is taken into account, assuming three configurations along height, namely "bare" (without infills), uniformly infilled and "pilotis" (without infills at the bottom storey) buildings. Two

(not code-based) Limit States are investigated, namely Usability-Preventing Damage, corresponding to an interruption of the building use, and Collapse.
RC elements are modelled with a lumped plasticity approach, through an empirical-based macromodel. The possible occurrence of shear failures in columns is taken into account through a preliminary classification of the expected failure mode (flexure- or shear-controlled, in the latter case prior to or following flexural yielding) and, if needed, a modification of the backbone of the nonlinear moment-chord rotation response, through empirical models providing the expected deformation capacity at shear and axial failure, the latter meant as the (initiation of) loss of axial-load-carrying-capacity. The nonlinear response of beam-column joints is modelled, too, with a "scissors model" based on concentrated springs representing the nonlinear response of the joint panel, at the intersection of beams' and columns' centerlines, through a preliminary evaluation of the expected failure mode (i.e. prior to or following yielding of adjacent beam/column elements). Materials properties are provided by literature studies, consistent with the age of construction of the buildings. The in-plane response of infills is modelled, taking into account the presence of openings, too. Modeling should be considered as simplified and, from some points of view, still preliminary, since advances are foreseen within the project in order to capture further failure modes that can occur in structural and nonstructural elements of older, nonductile RC buildings.
Nonlinear static analyses, allowing to identify the (top) displacement capacity at the investigated Limit States, are carried out. Multiple stripe nonlinear time history bi-directional analyses of the three-dimensional structural models are carried out in order to evaluate the demand, for ten stripes – each corresponding to a return period ranging from 10 to 10^5 years – and for twenty couples of records for each stripe. Records were selected, within the activities of the research project, based on a Probabilistic Seismic Hazard Analysis at the sites of interest for the selected return periods. Results are illustrated, highlighting the role of a – although obsolete – seismic design in the response of the buildings and in their capacity, more specifically in terms of displacement capacity at Collapse, but also in terms of demand estimated from multiple stripe analyses. Finally, demand-to-capacity ratios at the investigated Limit States are analyzed, which allow, within the scope of the project, the assessment of the seismic risk of the case study structures.

Keywords: Reinforced Concrete, Italian existing buildings, non-ductile, beam-column joints, masonry infill panels, Multiple Stripe Analysis.

1 INTRODUCTION

The RINTC project [1] is aimed at evaluating the seismic risk of buildings conforming to the Italian building code [2-3]. Different structural typologies are investigated (unreinforced masonry and base isolated RC residential buildings, precast RC and steel industrial buildings). The aim is assessing and comparing the risk of "collapse" and "damage" (as will be defined in the following) of the buildings. The project is currently ongoing, focusing – also – on the risk assessment of existing buildings, allowing to evaluate how suck a risk changed, during the time, based on the evolution of seismic codes and design practice.

In this study, the (preliminary, and currently ongoing) analysis of the seismic response of existing Italian residential RC buildings is reported, illustrating, first of all, the criteria adopted to select and design the case-study structures, the modeling strategy adopted for structural and non-structural elements typical of such a kind of structures, the investigated Limit States and, finally, the results of nonlinear static (pushover) and nonlinear time history (NLTH) multi-stripe analyses (MSAs).

The investigated structures are three-storey buildings, designed for gravity loads only during 1970s (gravity load designed, GLD) – located in three different sites, namely Milan, Naples and Catania, in increasing order of seismic hazard – or for moderate seismic loads during 1990s (seismic load designed, SLD) – located in L'Aquila. The simulated design of these structures is carried out consistent with code provisions and design practice at the time of interest. The presence of masonry infill nonstructural elements is considered, assuming three different configurations (frames with uniformly distributed infills along the height, frames with an open ground storey without infills, and, for comparison frames without infills). The modeling approach adopted for structural and nonstructural elements is basically consistent with the approach adopted to investigate the response of new structures, within the same project [4], but with modifications necessary to take into account and model the possible onset of non-ductile failure modes that were avoided in new structures by the application of capacity design (and, specifically, of strength hierarchy) principles in the design phase, namely in beam-column joints and in beam/column elements expected to experience a shear failure, prior to or following flexural yielding. The assumed Limit States are defined consistent with the response analysis of new structures, corresponding to Global Collapse (meant as non-conventional, "true" collapse condition) and Usability-Preventing Damage (corresponding to a damage level leading to building use interruption for repair); consistent with modeling assumptions, failure criteria at Global Collapse are modified, too, respect to new structures, in order to account for possible local failures in non-ductile structural elements. The (displacement) capacity at these Limit States is evaluated from pushover analyses; the demand is evaluated from NLTH MSAs, performed for ten stripes, corresponding to return periods from 10 to 10^5 years. Finally, the obtained demand-to-capacity ratios at the two Limit States, for the ten assumed return periods, are analyzed and compared, depending on the type of building (GLD or SLD) and the site hazard.

2 SELECTION OF CASE-STUDY STRUCTURES

Within the RINTC project, a set of case-study existing RC buildings to be analyzed in 2019-2021 has been established. The structures selected to this aim belong to a range of construction age from 1950s to 1990s, during which more than 80% of the Italian RC building stock was built, according to ISTAT census data [5]. As far as the type of design is concerned (i.e., for gravity loads only (GLD) or for seismic loads (SLD)), within this time range the areas classified as seismic gradually increased, particularly between 1980 and 1984, following the 1980 Irpinia earthquake [6]. At the same time, an evolution of technical codes was observed, too, with a major change – regarding seismic design provisions – represented by D.M. 3/3/1975 [7], that

introduced for the first time in Italy design criteria explicitly based on the dynamic properties of the structures, including, for instance, the so-called "inverted triangular" lateral force distribution. During this period, a change was observed also in the typology of steel reinforcement (i.e., plain or deformed), that influences significantly the deformation mechanisms ad, more generally, the response of RC structural elements under seismic action; a gradual transition from plain to deformed bars was observed around 1970s [8]. Based on these considerations, the structures to be analyzed, deemed as representative of the existing RC building stock, have been selected, corresponding to three time sub-ranges (1950s-60s, 1970s, 1980s-90s), assuming in all cases GLD and SLD design typologies, and with plain reinforcement in the first sub-range and deformed in the remaining two (see Table 1). For SLD buildings, a second seismic category, corresponding to a "moderate" seismic design level – and also, generally speaking, the most widespread in seismic areas in Italy in the periods of interest [6], is adopted. For each combination of these parameters (i.e., each row in Table 1) three- and six-storey buildings will be analyzed. GLD buildings will be analyzed at the sites of Milan, Naples and Catania, in increasing order of seismic hazard, while the SLD buildings will be designed and analyzed at the site of L'Aquila [9].

Type	Seismic category	Construction age	Type of reinforcement
GLD	-	1950s-60s	plain
		1970s	deformed
		1980s-90s	deformed
SLD	II	1950s-60s	plain
		1970s	deformed
		1980s-90s	deformed

Table 1: Summary of case-study existing buildings for the 2019-2021 RINTC project.

In this paper, preliminary results of first analyses on three-storey buildings, designed for gravity loads only (GLD) during 1970s or for moderate seismic loads (SLD) during 1990s, are reported.

In the following, the main characteristics of these case-study buildings, from the adopted layout, to the simulated design process, to main structural elements' characteristics, are described.

The case-study buildings have the same in-plan layout, with rectangular shape (total dimensions 21.4 x 11.8 m^2), five bays along the X direction and three in the Y one (Fig 1). The same plan layout was assumed for the new buildings previously analyzed during the project. In elevation, three-storey types (representative of low-rise buildings) have been considered (Fig 2). Inter-storey height is equal to 3.40 m for the first level and 3.05 for the others. Staircase substructure with knee beams is in symmetric position in relation to the Y direction.

Three infill configurations along the perimeter frames have been considered according to Bare Frame (BF, no effective infill is present), Infilled Frame (IF, infills uniformly distributed along the height) and Pilotis Frame (PF, no infill panels at the ground floor).

Different lateral resisting configurations have been designed for the two considered types (i.e. GLD and SLD). In particular, coherently to usual design practice, GLD types have frames in only one direction (i.e. orthogonal to the slab direction, Y). On the contrary, according to the code in force in the period, SLD types have lateral resisting frames along the two in-plane directions.

Section dimensions and reinforcement details have been evaluated by means of a simulated design [10] according to code prescriptions in force in Italy, i.e. D.M. 30/5/1974 [11] for GLD types and D.M. 14/2/1992 [12], as technical code, and D.M. 24/1/1986 [13], for seismic load provisions, for SLD types.

For both types, internal force related to gravity loads have been computed on the basis of the characteristic values of dead and live loads, these latter equal to 2.0 kN/m^2 as prescribed for residential buildings. Horizontal loads related to the second category (S=9 [13]) have been also considered in the design of SLD types.

For GLD, the simplified model of continuous beam resting on simple supports has been adopted in the analyses of beams, while columns have been designed by considering axial load only.

Following the common professional practice, SLD types have been designed by a linear elastic 3D model with fixed base and rigid diaphragm constraints at floors. No section stiffness reduction due to cracking has been considered. The design for seismic loads was carried out adopting a linear static analysis method.

The allowable stress method has been adopted in the safety verifications, considering medium quality concrete (Rck250, maximum allowable stress equal to 8.5MPa). Regarding steel mechanical properties, FeB38k (maximum allowable stress equal to 1,900 MPa) and Feb44k (maximum allowable stress equal to 2,600 MPa) deformed steel have been adopted for GLD and SLD types, representing the most adopted during 1970s and during 1980-90s, respectively [8].

As a result of the simulated design carried out for GLD types, cross-section dimensions of the interior flexible beams are 70 x 25 cm^2 and 100 x 25 cm^2 while, for SLD, they are 60 x 25 cm^2 and 80 x 25 cm^2. Perimeter beams are rigid beams with section dimension equal to 30 x 50 cm^2 for both GLD and SLD types.

Cross-section dimensions of columns are constant along the building height (30 x 30 cm^2) for GLD types, while they are equal to 30 x 40 cm^2 at the first/second level and 30 x 30 cm^2 at the third one for SLD.

Regarding reinforcement details, as a consequence of the minimum requirements provided in the above-mentioned Italian code, GLD columns have four reinforcement bars with diameter equal to 12 mm at each level while the stirrups' spacing is 25 cm. Longitudinal reinforcement ratio is between 0.37 and 0.75% in flexible beams and 0.15-0.37% for rigid ones. Transverse reinforcement is made up of 6 mm hoops with constant spacing equal to 17 and 25 cm for flexible and rigid beams, respectively. For SLD buildings, the longitudinal reinforcement ratio in columns is between 0.75 and 1.90%, between 0.40 and 1.26% in flexible beams, and between 0.27 and 0.67% in rigid beams. Transverse reinforcement is made up of 8 mm hoops with constant spacing between 12 and 15 cm in columns, between 7 and 17 cm in flexible beams, and between 13 and 19 cm in rigid beams.

With respect to infills, consistent with the practice of the period, double-layer type with 8 cm (internal layer) and 12 cm (external layer) thick panels of hollow clay bricks and empty cavity (10 cm thick) has been considered.

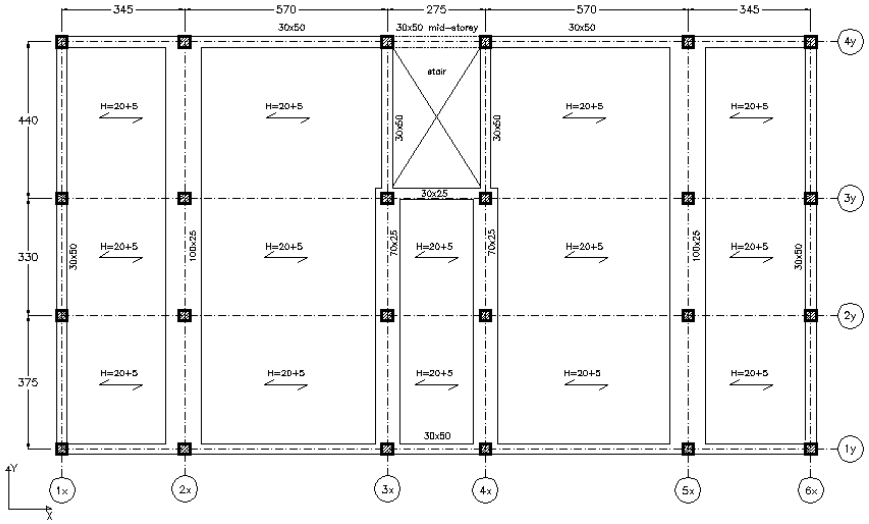

a)

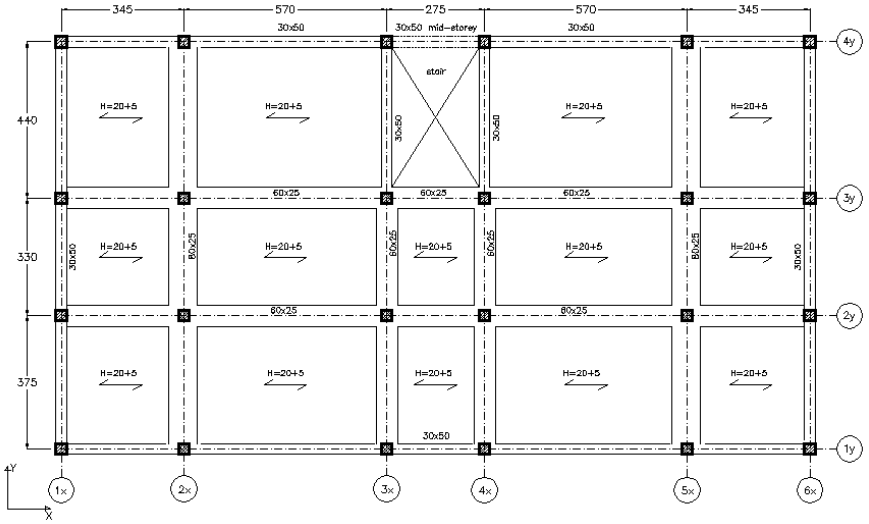

b)

Figure 1: Floor plan for GLD (a) and SLD (b) types.

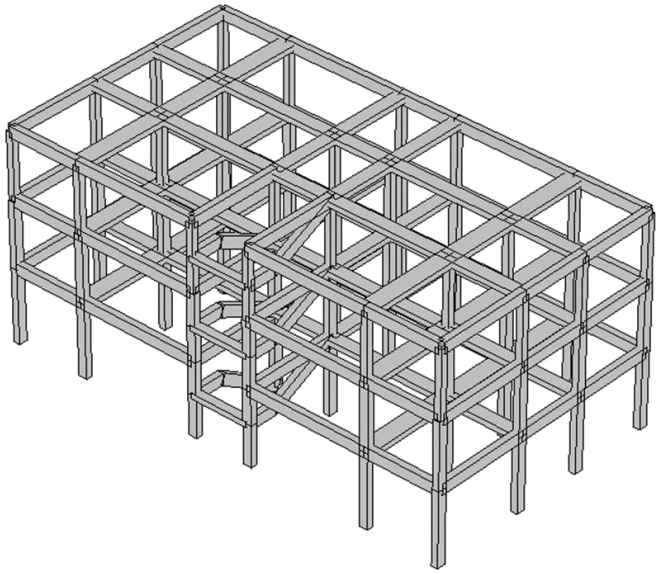

Figure 2: Three-dimensional view of the three-storey SLD building.

3 MODELING

The modeling approach adopted for RC and infill elements starts from the approach previously adopted for new buildings [1, 4], consistent with the literature state-of-the-art on these topics, but with simplifications representing a reasonable compromise with the computational demand due to the execution of several NLTH bi-directional analysis on 3D numerical models. Moreover, some modifications and integrations were necessarily adopted, in order to take into account specific failure mechanism that, contrary to new buildings, are not avoided by the adoption of capacity design principles, i.e., the possible onset of shear failures, prior to or following flexural yielding, in beam/column elements and in beam-column joints.

3.1 Beam/column elements

A lumped plasticity approach is adopted to model the nonlinear response of RC beam/column elements. Moment-chord rotation springs are introduced at both ends of each beam/column elastic element. The modified Ibarra-Medina-Krawinkler deterioration model with peak-oriented hysteretic response (ModIMKPeakOriented Material in OpenSees [14]) with response parameters determined according to [15] is assigned to such springs. The empirical nature of the model, whose predictive equations are derived based on a great number of experimental results, allows reproducing accurately and reliably the softening behaviour of RC elements as well as strength and stiffness degradation due to cyclic loading. This is a key issue when investigating the seismic response of RC framed structures up to global collapse, as done in this study. This is the main advantage of adopting Haselton et al.'s empirical equations for modelling the lateral response of RC elements. It "counterbalances" the well-known inherent limitations of the lumped plasticity approach adopted, namely the absence of coupling and interaction between axial load and bidirectional bending moments as well as the assumption of constant axial load and shear length when determining RC elements' response parameters. Further details are reported in [4].

The empirical formulations by Haselton et al. were determined with reference to a wide database of RC columns with both ductile and "limited" ductile response. Nevertheless, to explicitly account for shear failures of elements during structural analyses and for their influence on the overall structural response, the predicted ductile backbone curves of elements detected as shear-critical based on a force-based simplified procedure were modified according to deformation limits at shear- and axial load-failure of shear-sensitive elements.

More specifically, the failure mode of members was pre-determined by comparing the maximum moment strength predicted by Haselton et al.'s model, M_{max}, and the yielding moment, M_y, divided by the element shear length, L_s, ($M_{max}/L_s=V_{max}$, $M_y/L_s=V_y$) with the maximum ($V_{R,max}$) and minimum ($V_{R,min}$) shear strength predicted by the well-established model by Sezen and Moehle [16]. If $V_{R,min}$ was higher than V_{max}, the element was recognized as "ductile". In all the other cases, the element was classified as shear-critical. Namely, if $V_{R,max}$ was lower than V_y, the element was recognized as "brittle". In all the other cases, the element was characterized by a flexure-shear interaction failure mechanism. The backbone predicted by Haselton et al.'s model for ductile elements was not modified. For shear-critical elements, the predicted backbone was modified by assuming the maximum lateral load strength at the attainment of the lateral displacement at shear failure, Δ_s, and then a softening branch up to zero lateral load resistance at the lateral displacement at axial failure, Δ_a. Δ_s and Δ_a were calculated based on the empirical proposal by Aslani and Miranda [17]. A schematic representation of the procedure adopted for failure mode classification and response backbone modification is reported in Figure 3. This approach was preferred to the one by Elwood and Moehle [18, 19] given that the empirical formulations proposed by Aslani and Miranda are defined in order to always provide Δ_a values greater than Δ_s.

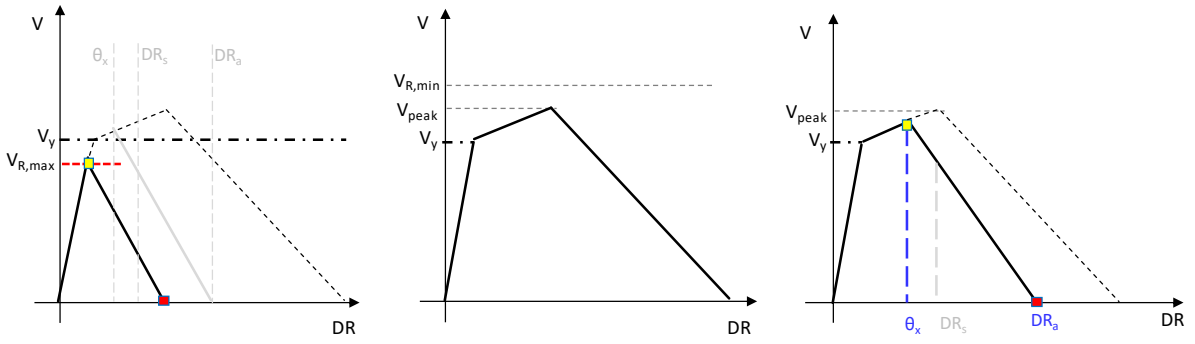

(a) (b) (c)

Figure 3: Schematic representation of the classification procedure and response backbone modification for RC columns: $V_{R,max}<V_y$, shear failure prior to flexural yielding (a); $V_{R,min}>V_{peak}$, flexural failure (b); all other cases, shear failure following flexural yielding (c).

In the literature, a consolidated unified approach for determining the failure mode of RC elements and, consistently, their consequent lateral response under cyclic loads is missing. Ongoing research is focused on this issue, see for example [20-22]. Given that, the hybrid approach used in this study seems to be the best compromise to account for the potential shear failure of structural elements without renouncing to the recognized reliability of Haselton et al.'s model in predicting the hysteretic response of RC members.

3.2 Beam-column joint elements

The joint panel model adopted herein is the so-called "scissors model" by Alath and Kunnath [23], a very simple and computationally less demanding joint model, but also sufficiently accurate in predicting the experimental beam-column joint panel behavior for simulating the seismic response of non-ductile RC frames [24]. The "scissors model" is implemented by defining rigid offsets spreading within the joint region and two duplicate nodes, node "A" and node "B", geometrically overlapped in the center of the joint panel (Figure 4a). Node A is connected to the columns rigid links and node B is connected to the beams rigid links. A *zero-length* rotational spring connects these two nodes allowing only relative rotation between them by means of a proper constitutive model, reproduced with the *Pinching4 uniaxial material* in OpenSees [14], as described in the Section. The joint rotational spring can be accurately defined through a quadri-linear moment (M_j) – rotation (Θ_j) relationship [24-27], strictly linked to the joint shear stress (τ_j) – shear strain (γ_j) response, and characterized by the following characteristic points (Figure 4b): cracking, pre-peak, peak and residual points.

The quadri-linear joint response for exterior unreinforced joints – both in terms of envelope definition and hysteretic behaviour – is defined herein as proposed in [24], based on experimental data reported in [28-30], for which experimental shear stress-strain relationships of joint panel were provided.

Similarly, for interior unreinforced joints, the $\tau_j - \gamma_j$ envelope proposed in Celik and Ellingwood [25] is adopted. About the hysteretic response of the interior joints, the cyclic degradation and pinching parameters calibrated by Jeon et al. [26] are assumed. However, these parameters are modified so that no strength degradation (parameters gF=0 in the *Piching4 material*) is taken into account, since strength degradation is already included in the backbone of the joint response obtained from experimental data.

Both for exterior and interior joints, the joint shear strength $\tau_{j,max}$ is predicted according to [26], namely as a function of joint typology (interior or exterior), concrete compressive strength, beam longitudinal reinforcement, and presence of transverse beams. This model showed a mean value of predicted-to-experimental strength ratio very close to the unit for a wide dataset [31]. Additionally, both for exterior and interior joints, the adopted constitutive model accounts for two possible failure mode of the beam-column joints: joint shear failure prior to (J-failure) or after (BJ/CJ-failure) the achievement of yielding of the adjacent beams/columns (in strong column-weak beam/weak column-strong beam hypothesis), both for exterior and interior joints.

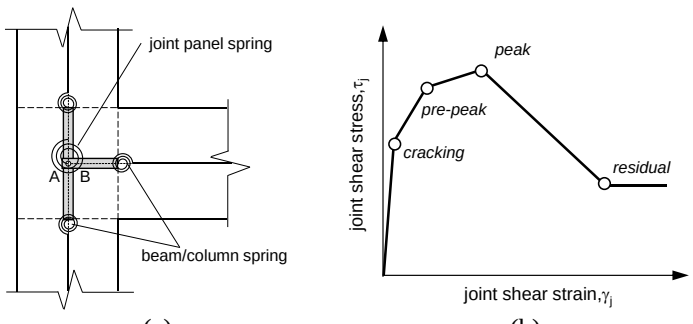

(a) (b)

Figure 4: Joint modelling approach for an exterior joint (a) and schematic of stress-strain envelope for the joint panel (b) – adapted from De Risi et al. [2016a].

In conclusion, for the joint panel spring definition, the deformability parameter "rotation" Θ_j coincides with the joint panel shear deformation (γ_j). For each characteristic point of the joint envelope, the moment transferred through the rotational spring, M_j, can be calculated as a function of the joint shear stress τ_j, as in [25] or [24], based on simple equilibrium equations.

3.3 Masonry infill elements

Double leaf 80+120 mm masonry infills are assumed. Consistent with the assumed architectural plan layout, different opening percentages are assumed in the panels, namely with solid panels along the Y direction and opening percentages roughly between 20 and 50% along the X direction. An equivalent concentric single-strut approach is adopted to represent the infill panels, following [32-34]. Within the RINTC project, data from [35-37] were elaborated in order to establish drift thresholds at cracking, peak, and collapse. The effect of openings is taken into account according to [33]. For further details, the reader is referred to [1] and [4].

3.4 Material properties

The mean concrete compressive strength and steel yield strength for the assessment were provided by literature studies on material properties of existing RC buildings in Italy. For concrete, the cylindrical compressive strength, f_c, is assumed equal to 20 and 25 MPa for GLD and SLD buildings, respectively, in order to be representative of RC buildings built during 1970s and during 1980-90s, respectively [38]. For steel, the yield strength, f_y, is assumed equal to 448 and 535 MPa for GLD and SLD buildings, respectively, in order to be representative of FeB38k commercial typology between 1974 and 1980, and of FeB44k commercial typology between 1990 and 1996, respectively [8]. For masonry infill panels, material properties are assumed in order to be representative of "light" nonstructural masonry, likely present in existing RC buildings, based on the data collected in [36], assuming a masonry compressive strength f_m=2 MPa, a masonry shear strength τ_{m0}=0.4 MPa, a basic shear strength of bed joints τ_0=0.27 MPa, and a modulus of elasticity E_m=1500 MPa.

4 LIMIT STATES AND FAILURE CRITERIA

The response of the case-study structures is assessed at two Limit States (LSs), namely "Global Collapse" (GC) and "Usability-Preventing Damage" (UPD), corresponding to the non-conventional, "true" collapse condition and to a damage level leading to building use interruption for repair, respectively. Further details are provided in [4]. As for the modeling approach, basically the definition of LSs was consistent with the approach previously adopted for new buildings, but, as far as the GC LS is concerned, with some modifications accounting for possible failure mechanism that can occur in structural elements of existing, "non-ductile" RC buildings. The definition of these LSs will be used in the evaluation of the corresponding displacement capacity from the results of nonlinear static (pushover) analyses, as will be shown in the next Section.

4.1 Global Collapse Limit State

The GC LS corresponds to the "true" collapse, meant as loss of structural integrity. Several definitions of building collapse are available in the literature, which lead to very different results [39]. At global level, in buildings with flexure-controlled structural elements, such a condition can be identified with dynamic instability, corresponding to the attainment of a sidesway collapse. This is the case of new buildings, as those previously analyzed within the RINTC project. The displacement capacity (from pushover analyses) corresponding to such a condition should be identified, in a single-mode pushover curve, at the zero-base shear condition; nevertheless, such condition is assumed to be "anticipated" at 50% base shear drop in order to account – approximately – for the strength degradation in RC beams/columns during inelastic cyclic response, which, within the adopted modeling approach [14], is captured during NLTHs but not

in pushover analyses [1, 4]. A slight modification to this approach has been subsequently assumed, within the RINTC project, in order to identify a displacement capacity corresponding to a strength degradation that could be attributed to structural elements only, and that is assumed herein and described as follows:

- The storey shear in RC elements (at storeys not "unloading" during the pushover analysis) attains 50% of peak in the descending branch of the storey shear-displacement curve.

Nevertheless, in existing, non-ductile RC buildings, the possible onset of brittle failures in structural elements makes it necessary to consider also another collapse mechanism, that corresponds loss of vertical-load-carrying-capacity in shear-controlled columns [17] or beam-column joints [40]. This kind of collapse is generated by the activation of a sliding mechanism along the diagonal crack surfaces that develop at the onset of the shear failure. The chord rotation (for shear-controlled columns) or the Interstorey Drift Ratio (IDR) (for beam-column joints) at "axial failure" are provided by empirical formulations proposed in literature studies [17, 40]. Nevertheless, strictly speaking, such deformation limits should be regarded as corresponding to the *initiation* of loss of axial-load-carrying-capacity; if the "true" local collapse is assumed to correspond to the complete loss of axial-load-carrying-capacity, higher values should be assumed, corresponding to a null axial-load-carrying-capacity [41, 42]. Both for shear-controlled columns and beam-column joints, based on the abovementioned studies, with some simplification, such deformation limits can be assumed equal to 0.10 (chord rotation or IDR, respectively). Hence, the following further criteria are assumed for the evaluation of the displacement capacity at GC LS:

- The first column classified as shear-controlled (prior to or following flexural yielding) reaches a chord rotation equal to 0.10;
- The storeys above and below the first beam-column joint failed (prior to or following flexural yielding of the adjacent beams/columns) reach a (average) IDR equal to 0.10.

4.2 Usability-Preventing Damage Limit State

The UPD LS corresponds to a damage level to structural or nonstructural elements leading to building use interruption for repair. Its definition makes it close to the code-based Damage Limitation LS. A multi-criteria approach is adopted in order to define this LS, reflecting two basic principles, i.e. that at the attainment of this LS (i) the structure has to show a moderate stiffness decrease, without strength decrease, and (ii) the nonstructural (infill) elements have to show an extent and a degree of damage such that repair is no more easily and economically feasible, leading to interruption of use. The abovementioned multi-criteria approach applies evaluating the displacement capacity (from pushover analyses) at this LS at the attainment of the first of the following conditions:

- Base shear attains 95% of peak in the ascending branch of the pushover curve, reflecting a "moderate" stiffness decrease;
- 50% of the infill panels reach their displacement at peak load, corresponding to a "cracking" damage condition; the correspondence between the attainment of the peak lateral force of the panel, of the usually called DS2 (extensive cracking) and of the code-based Damage Limitation LS is commonly accepted in literature [35, 37, 43-47];
- The first infill panel reaches its displacement at 50% strength degradation, corresponding to a "severe" damage condition.

For BFs, that represent a non-realistic numerical reference model, a different approach is adopted, assuming the maximum IDR as Engineering Demand Parameter (EPD), and the code-based 0.5% limit for capacity, with "local" checks in post-processing of NLTH analyses.

For further details, the reader is referred to [1] and [4].

5 PUSHOVER ANALYSIS RESULTS

In this Section, the results of the nonlinear static (pushover) analysis carried out on the case-study buildings are reported. Pushover analyses are carried out with two different lateral force patterns, i.e. "modal" and "uniform" (or "mass-proportional"). The displacement capacity is evaluated from the curves obtained with a lateral force pattern proportional to an assumed deformed shape (corresponding to the first mode of vibration or uniform) closer to the actual, observed deformed shape at the attainment of the LS condition. In particular, as a consequence of a storey mechanism at collapse generally found for both GLD and SLD types, the uniform load pattern is adopted to evaluate the GC displacement capacities.

Results are reported in terms of Roof Drift Ratio (RDR) versus ratio between the base shear (V) and the building weight (W). Figures 5 and 6 report the pushover curves of GLD and SLD buildings, respectively. Note that pushover curves in along X are reported only for positive pushing direction, because, due to structural symmetry, data for negative pushing direction are nearly identical.

Generally speaking, a significantly higher base shear capacity is observed for SLD buildings, as clearly expected, with a V/W ratio, for BFs, roughly between 0.20 and 0.35, in X and Y direction, compared to GLD buildings, that show a V/W ratio roughly between 0.10 and 0.20. The influence of infill panels, in terms of stiffness/strength increase compared to BFs, is clear particularly for IFs, but – except for GLD buildings in X direction – is not as significant for PFs. This is consistent with the soft-storey collapse mechanism that is observed in nearly all cases.

The RDR capacity at UPD and GC is reported on the pushover curves from which it was evaluated. More specifically, at GC both the "global" capacity (corresponding to the attainment of 50% of peak in the descending branch of the storeys' RC shear-displacement curves) and the capacity corresponding to column axial failure (corresponding to the attainment of 0.10 chord rotation in the first column classified as shear-controlled) are reported; the lowest governs the attainment of GC. The axial failure of a beam-column joint (corresponding to the attainment of 0.10 IDR) is never observed. Except for GLD BF buildings in Y direction, the column axial failure does not govern the attainment of GC, that is – instead – generally governed by the attainment of the "global" collapse condition. Such a capacity is generally significantly higher for SLD buildings.

Note that for BF buildings, the EDP at UPD is the maximum IDR and the capacity is the code-based 0.5% IDR limit. Only for comparison purposes with the IFs and the PFs (where the top displacement is the EDP), the RDR in the pushover curves corresponding to the attainment of a maximum IDR equal to 0.5% is reported. For GLD IF and PF buildings, the attainment of UPD is controlled, in all cases, by the 95% base shear condition. For SLD IF and PF buildings, the attainment of UPD is controlled by the 95% base shear condition in Y direction, and by the attainment of displacement at peak load in 50% of the infill panels in X direction. Contrary to GC, at UPD there is not a clear hierarchy between the capacity of GLD and SLD buildings.

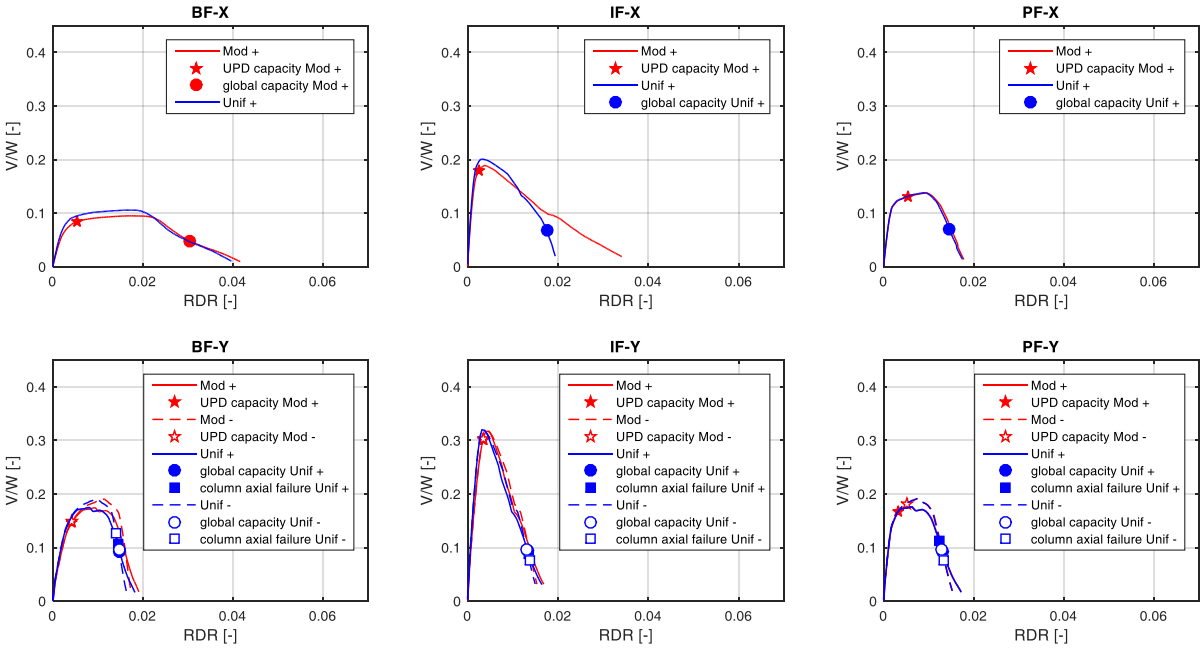

Figure 5: Pushover curves of the three-storey GLD buildings.

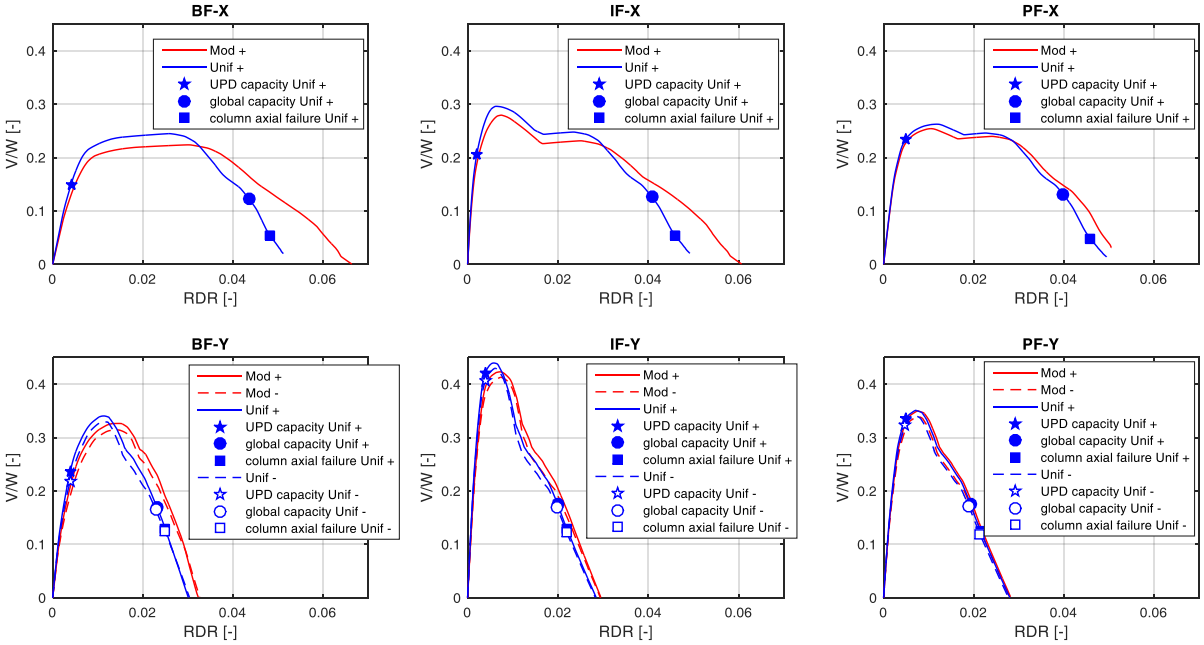

Figure 6: Pushover curves of the three-storey SLD buildings.

Type	Infill configuration	Direction [X/Y]	UPD [RDR]	GC (global) [RDR]	GC (c.a.f.) [RDR]
GLD	BF	X	0.0053	0.0305	-
		Y	0.0043	0.0144	0.0143
	IF	X	0.0025*	0.0176	-
		Y	0.0034*	0.0133	0.0136
	PF	X	0.0055*	0.0146	-
		Y	0.0033*	0.0123	0.0129
SLD	BF	X	0.0041	0.0433	0.0480
		Y	0.0039	0.0230	0.0249
	IF	X	0.0020**	0.0405	0.0460
		Y	0.0039*	0.0198	0.0220
	PF	X	0.0048**	0.0396	0.0459
		Y	0.0049*	0.0191	0.0215

* attainment of 95% base shear condition

** attainment of displacement at peak load in 50% of the infill panels

Table 2: RDR capacity at UPD and GC for the case-study buildings (values in grey do not govern the capacity at GC). For GC, the values evaluated for both global collapse (global) and column axial failure (c.a.f,) are separately reported.

6 MULTIPLE STRIPE ANALYSIS RESULTS

The results of MSAs carried out on the case-study structures are illustrated in this section. MSAs were performed with NLTH bi-directional analyses for ten stripes, corresponding to increasing ground motion return periods ranging from 10 to 10^5 years and for 20 couples of records in each stripe [9]. The conditioning intensity measure (IM) for record selection was the spectral pseudo-acceleration with 5% damping at the vibration period T, $S_a(T)$. T was selected between {0.15, 0.5, 1.0, 1.5, 2.0} sec, as the closest to the fundamental period of vibration of the building (see Table 3); 1.0, 0.5 and 0.5 sec were chosen for BF, IF and PF buildings, respectively, both for GLD and SLD types.

Type	Infill configuration	T [sec]
GLD	BF	0.93
	IF	0.46
	PF	0.66
SLD	BF	0.86
	IF	0.44
	PF	0.66

Table 3: Fundamental period of vibration of the three-storey case-study buildings.

Figure 7 reports the RDR demand for the case-study structures, i.e. the three-storey GLD (located in Milan, Naples and Catania) and SLD (located in L'Aquila) buildings in BF, IF and PF configurations. Similar RDR demands are generally observed for IF and PF buildings, and slightly higher for BF. Except for Milan, a high number of dynamic instability cases is observed, especially for Catania site. Specifically, if RDR demands for GLD buildings are analyzed, it can be observed that dynamic instability occurs in nearly all cases if an RDR about equal to 0.01 (for IF and PF) or slightly higher (for BF) is attained; this is consistent with results of pushover analyses and with the assumed "global" capacity values at GC. The same occurs for

SLD buildings for an RDR about equal to 0.03. As expected, a clear increase in demand with increasing site hazard is observed for GLD buildings in Milan, Naples and Catania.

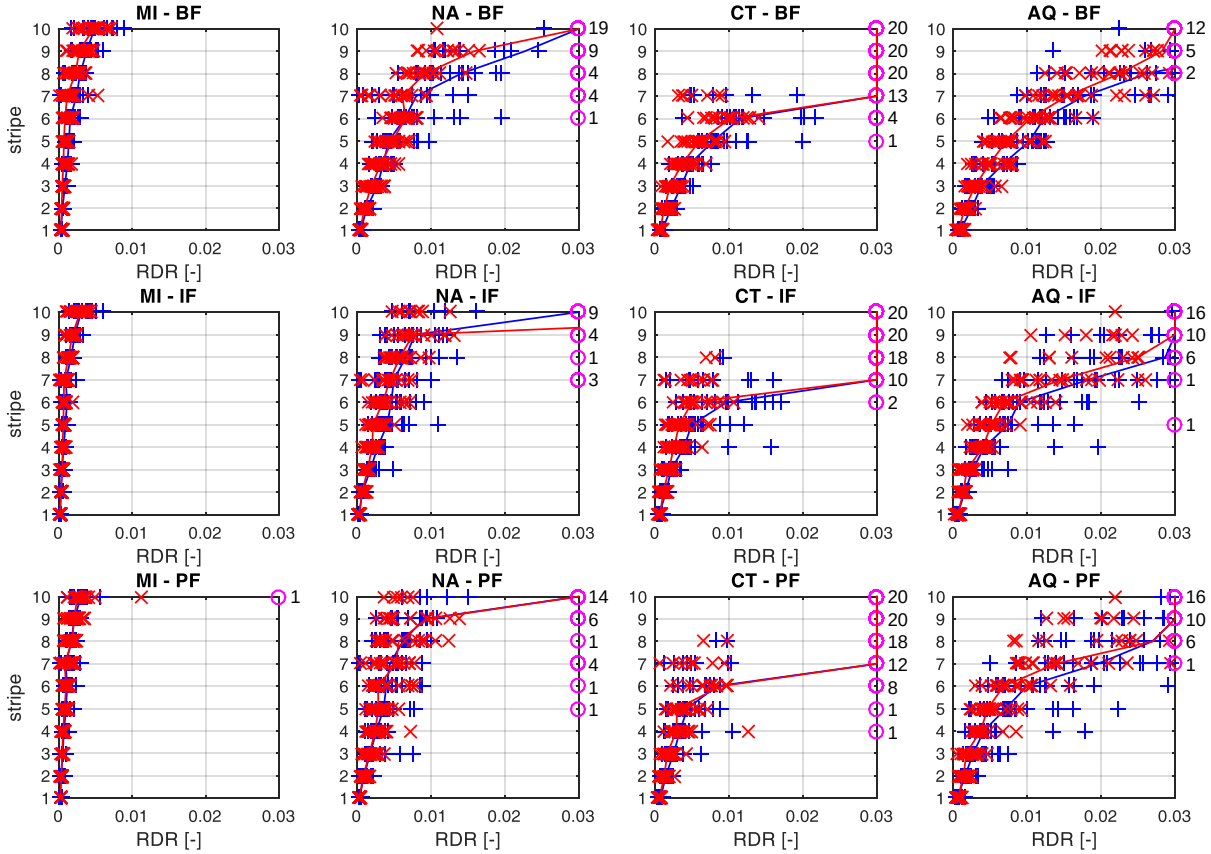

Figure 7: RDR demands from MSAs on MRF buildings in Milan, Naples, Catania and L'Aquila, soil C. Blue and red solid lines connect the median values of RDR demand at each stripe, in X and Y directions, respectively. A higher stripe number corresponds to higher return periods, from 10 to 10^5 years [9]. Numbers close to pink circles represent dynamic instability cases.

The influence of the type of design (GLD and SLD) on the RDR demand can be observed more clearly analyzing the median RDR demand in X and Y directions as a function of the conditioning IM, i.e. the elastic spectral pseudo-acceleration at the selected period of vibration, $S_a(T)$, see Figure 8. Such a direct comparison (between different sites, for each infill configuration) is possible because the same period of vibration was selected – and thereby the same conditioning IM was assumed – for GLD and SLD buildings, given equal the infill configuration. If the results of the SLD buildings in L'Aquila are compared with the GLD buildings in Catania (characterized by a quite similar hazard), a slightly lower demand, especially for higher $S_a(T)$ values, can be observed for SLD buildings.

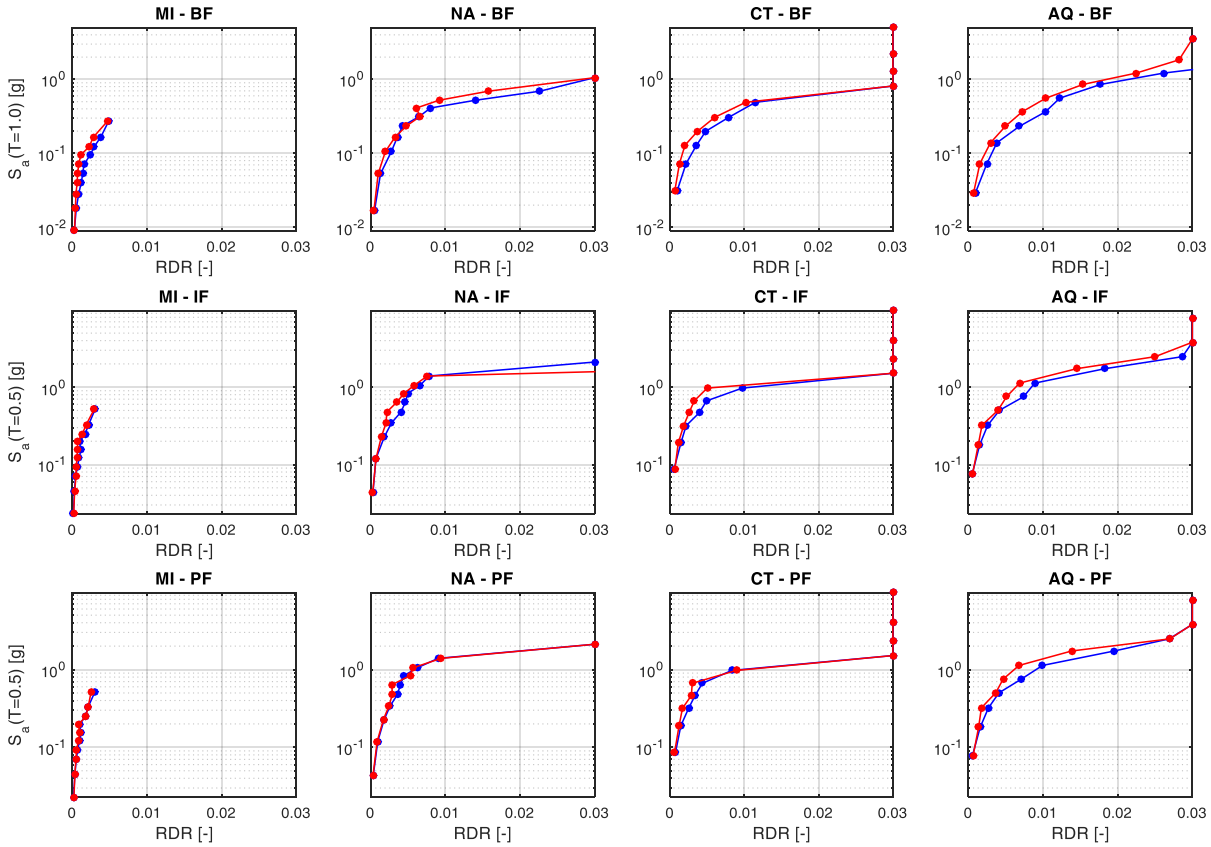

Figure 8: median RDR demands from MSAs on MRF buildings in Milan, Naples, Catania and L'Aquila, soil C, depending on the elastic spectral pseudo-acceleration at the selected period of vibration. Blue and red represent X and Y directions, respectively. Each dot corresponds to a stripe. Median RDR demand values higher than 0.03 are conventionally reported at 0.03.

In the following, the demand-to-capacity (D/C) ratios at GC are reported for the case-study structures. Specifically, Figure 9 reports the D/C ratio value for each stripe while the median, evaluated as the maximum value between X and Y direction, is shown in Figure 10. In the same figure, the median value is plotted as a function of $S_a(T)$.

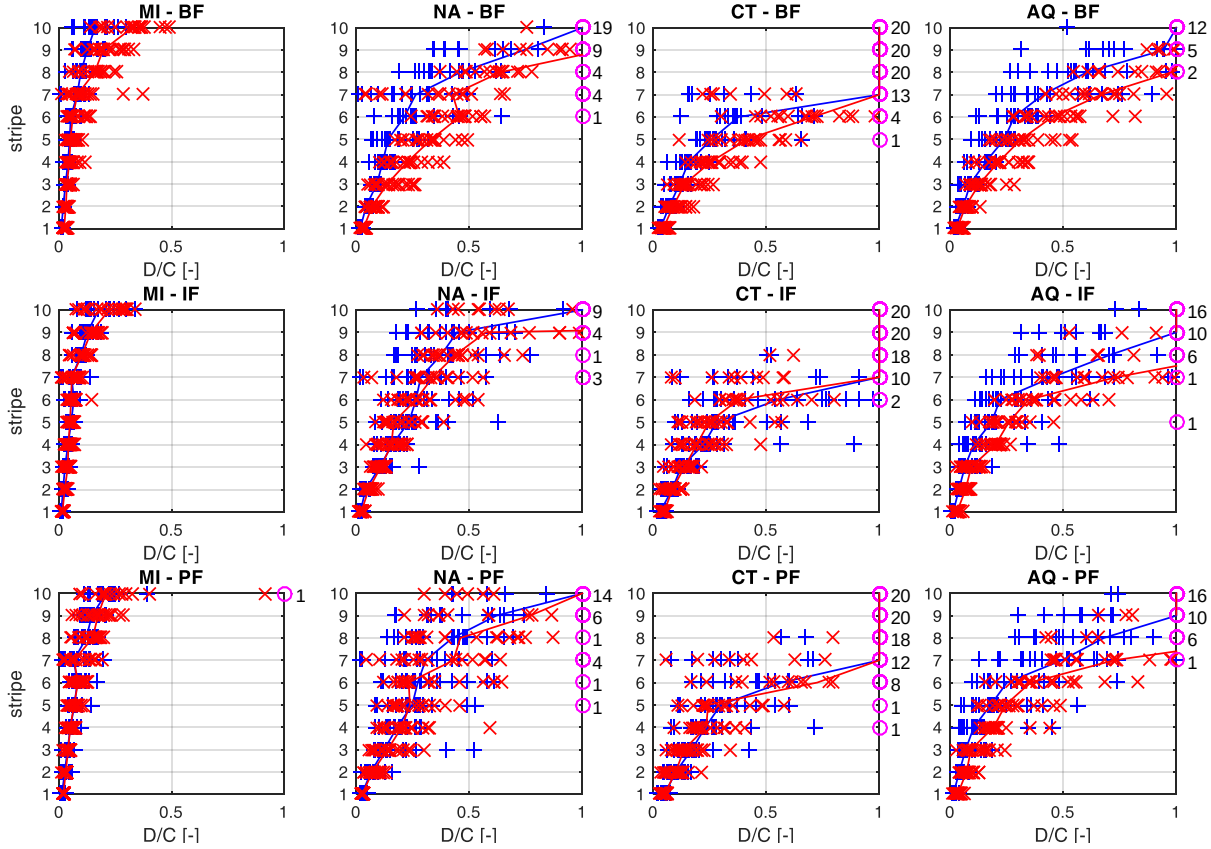

Figure 9: D/C ratios at GC for MRF buildings in Milan, Naples, Catania and L'Aquila, soil C. Blue and red solid lines connect the median values of D/C ratio at each stripe, in X and Y directions, respectively. A higher stripe number corresponds to higher return periods, from 10 to 10^5 years [9]. Numbers close to pink circles represent dynamic instability cases.

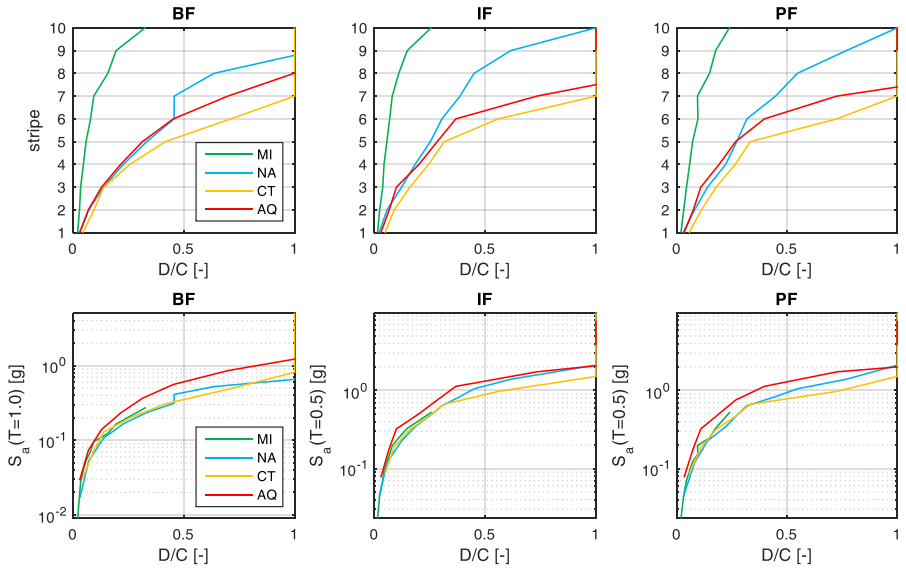

Figure 10: median D/C ratios (maximum between X and Y direction) at GC depending on stripe number (top row) and elastic spectral pseudo-acceleration at the selected period of vibration, $S_a(T)$ (bottom row).

At GC, if dynamic instability is not observed, the D/C ratio is generally lower than 1. As far as the influence of the type of design is concerned, if Catania (GLD) and L'Aquila (SLD) sites

– that are characterized by a quite similar hazard, and by a demand slightly lower for SLD buildings in L'Aquila – are compared, the significantly higher capacity of SLD buildings leads to lower D/C ratio values. For each site, PF type generally show a greater number of dynamic instability than IF one, thus highlighting the high vulnerability of buildings in case of infills irregularly arranged along the height.

A more straightforward comparison can be carried out reporting for all sites the median (of the maximum between X and Y direction) D/C ratio values depending on the stripe number and of the conditioning IM, i.e. the elastic spectral pseudo-acceleration at the selected period of vibration, $S_a(T)$. Specifically, from the $S_a(T)$-D/C ratio relationships, the lower values D/C – given equal the $S_a(T)$ – for SLD buildings (L'Aquila), compared to GLD, can be observed. As far as GLD buildings are concerned, a very similar behavior – as expected – from site to site (Milan, Naples, Catania) is observed.

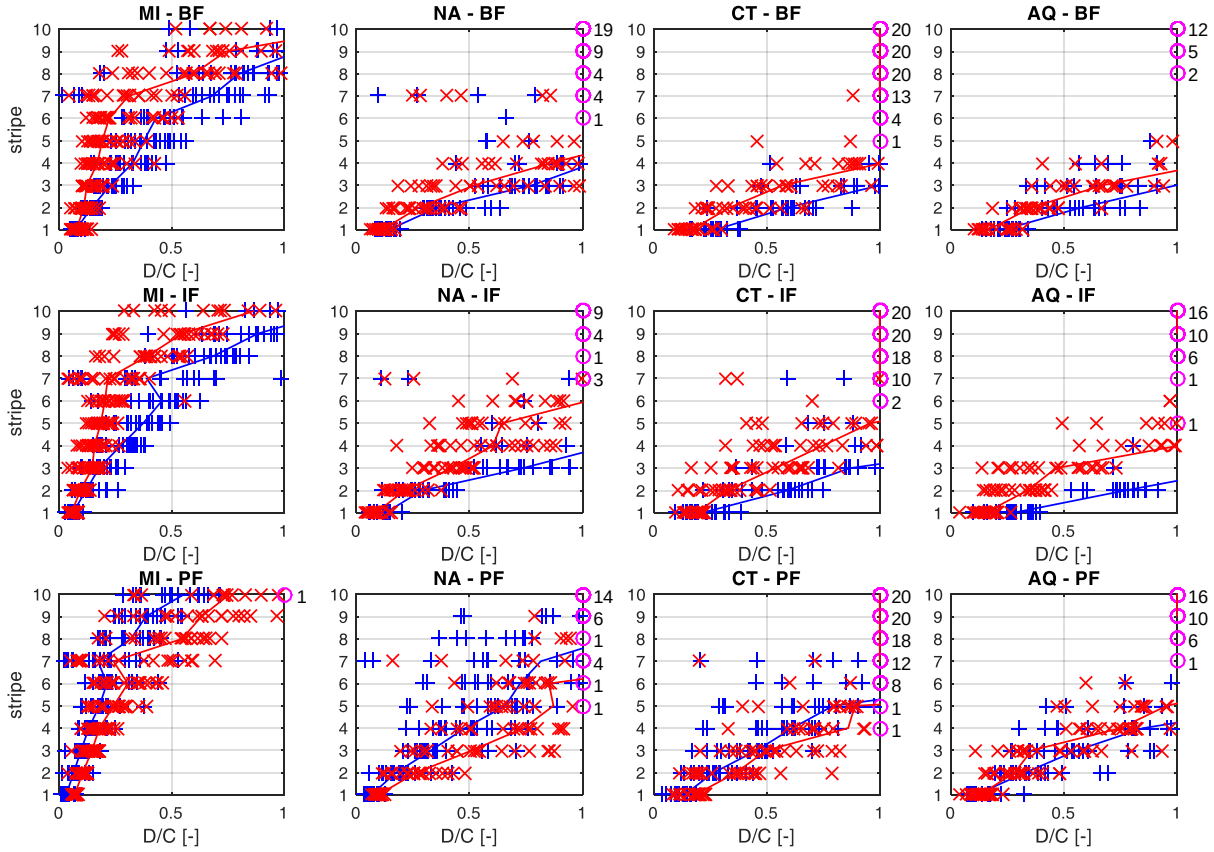

Figure 11: D/C ratios at UPD for MRF buildings in Milan, Naples, Catania and L'Aquila, soil C. Blue and red solid lines connect the median values of D/C ratio at each stripe, in X and Y directions, respectively. A higher stripe number corresponds to higher return periods, from 10 to 10^5 years [9]. Numbers close to pink circles represent dynamic instability cases.

As for the GC LS, Figures 11 and 12 show the results obtained for the UPD LS. First of all, due to the absence in the seismic code of specific prescriptions devoted to non-structural damage prevention, slight differences between GLD and SLD results can be observed, i.e. from Catania to L'Aquila (which are characterized by a quite similar hazard). For GLD, the D/C ratios basically reflect the site hazard, with increasing values from Milan to Naples and Catania.

Further, although GLD types were designed only for vertical loads, UPD LS in Milan is achieved for very high intensities, e.g. stripe #9 for IF type, 10^4 years return period.

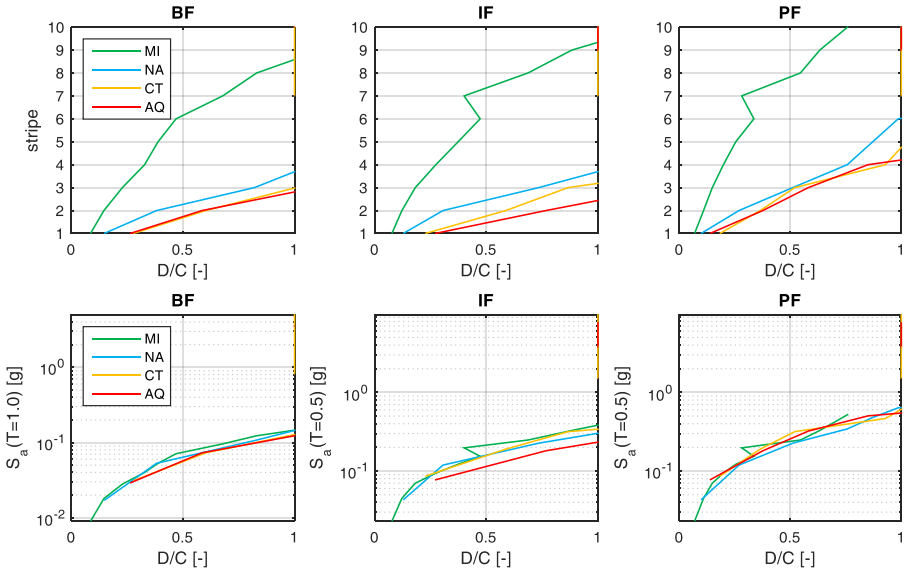

Figure 12: median D/C ratios (maximum between X and Y direction) at UPD depending on stripe number (top row) and elastic spectral pseudo-acceleration at the selected period of vibration, $S_a(T)$ (bottom row).

7 CONCLUSIONS

In this paper, preliminary results of the first analyses carried out on existing RC buildings representative of the Italian buildings stock within the RINTC project were illustrated. The procedure for selecting the case-study structures and the simulated design process are described. Three-storey GLD and SLD buildings were analyzed, the former located in Milan, Naples and Catania, the latter in L'Aquila. The modeling approach, basically consistent with the approach previously adopted within the project for new buildings, based on lumped plasticity with a phenomenological macromodel for RC elements and on an equivalent strut approach for infill panels, was modified and developed in order to take into account specific damage/failure mechanisms of non-ductile structural elements, such as the modeling of beam-column joints' response, by means of a "scissors model", and the displacement-based modeling of shear failures in frame elements. Failure criteria were properly integrated in order to take into account, specifically, possible local collapses due to the loss of vertical-load-carrying-capacity in shear-controlled elements.

The evaluation of the displacement capacity at the two considered LSs, i.e. GC and UPD, based on pushover analyses, showed that at GC the attainment of the LS capacity was governed by a "global" collapse – meant as corresponding to the onset of dynamic instability – instead of a "local" collapse, due, above all, to the adoption of a collapse definition for shear-controlled frame elements (and beam-column joints) that does not correspond to the initiation, but, instead, to the complete loss of vertical-load-carrying-capacity. SLD buildings showed a significantly higher displacement capacity at GC, and thereby, for a similar hazard, significantly lower D/C ratio values compared to GLD buildings. At UPD, instead, no clear influence of the type of design was observed.

During the next years of the project, further case-study buildings will be modelled and analyzed, providing a complete framework of data on structures representative of the existing RC building stock. Furthermore, the modeling approach will be developed, in order to take into

account of phenomena such as, among others, of the out-of-plane response of masonry infill panels and the in-plane local interaction between masonry infill panels and structural elements.

REFERENCES

[1] RINTC Workgroup. Results of the 2015-2017 implicit seismic risk of code-conforming structures in Italy (RINTC) project. ReLUIS report, Rete dei Laboratori Universitari di Ingegneria Sismica, Naples, 2018. Available at http://www.reluis.it/

[2] NTC2008. Decreto ministeriale 14 gennaio 2008 - Norme Tecniche per le Costruzioni. Supplemento ordinario n. 30 Gazzetta Ufficiale 4 febbraio 2008, n. 29. 2008. (in Italian).

[3] NTC2018. Decreto ministeriale 17 gennaio 2018 – Aggiornamento delle "Norme Tecniche per le Costruzioni". Supplemento ordinario n. 8 Gazzetta Ufficiale 20 febbraio 2018, n 42. 2018. (in Italian).

[4] P. Ricci, V. Manfredi, F. Noto, M. Terrenzi, C. Petrone, F. Celano, M.T. De Risi, G. Camata, P. Franchin, G. Magliulo, A. Masi, F. Mollaioli, E. Spacone, G.M. Verderame. Modeling and seismic response analysis of Italian code-conforming reinforced concrete buildings. *Journal of Earthquake Engineering*, **22**(S2), 105-139, 2018.

[5] ISTAT. 15° Censimento generale della popolazione e delle abitazioni. Istituto Nazionale di Statistica, Rome, Italy, 2011. (in Italian).

[6] C. Del Gaudio, P. Ricci, G.M. Verderame. ECS-it – Evoluzione della classificazione sismica in Italia. ReLUIS, Naples, Italy, 2015. Available at http://www.reluis.it/

[7] DM75. Decreto Ministeriale n. 40 del 3 marzo 1975. Approvazione delle norme tecniche per le costruzioni in zone sismiche. Gazzetta Ufficiale 8 aprile 1975 n. 93. 1975. (in Italian)

[8] G.M. Verderame, P. Ricci, M. Esposito, G. Manfredi. STIL v1.0 – Software per la caratterizzazione delle proprietà meccaniche degli acciai da c.a. tra il 1950 e il 2000. ReLUIS, Naples, Italy, 2012. Available at http://www.reluis.it/

[9] I. Iervolino, A. Spillatura, P. Bazzurro. RINTC-E project: towards the assessment of the seismic risk of existing buildings in Italy. *7th International conference on computational methods in structural dynamics and earthquake engineering – COMPDYN 2019*, Crete, Greece, June 24 – 26, 2019.

[10] A. Masi. Seismic vulnerability assessment of gravity load designed R/C frames. *Bulletin of Earthquake Engineering*, **1**(3), 371-395, 2003.

[11] Decreto Ministeriale 30 maggio 1974. Norme tecniche per la esecuzione delle opere in cemento armato normale e precompresso e per le strutture metalliche. Gazzetta Ufficiale n. 198 del 29 luglio 1974. (in Italian).

[12] Decreto Ministeriale 14 febbraio 1992. Norme tecniche per le opere in c.a. normale e precompresso e per le strutture metalliche. Gazzetta Ufficiale n. 65 del 18 marzo 1992. (in Italian).

[13] Decreto Ministeriale 24 gennaio 1986. Norme tecniche relative alle costruzioni antisismiche. Gazzetta Ufficiale n. 108 del 12 maggio 1986. (in Italian).

[14] F. McKenna, G.L. Fenves, M.H. Scott. Open system for earthquake engineering simulation. University of California, Berkeley, CA, 2000.

[15] C.B. Haselton, A.B. Liel, S.T. Lange, G.G. Deierlein. Beam-column element model calibrated for predicting flexural response leading to global collapse of RC frame buildings. Pacific Earthquake Engineering Research Center, Report 2007/03, Berkeley, California, USA, 2008.

[16] H. Sezen, J.P. Moehle. Shear strength model for lightly reinforced concrete columns. *Journal of Structural Engineering*, **130**(11), 1692-1703, 2004.

[17] H. Aslani, E. Miranda. Probabilistic earthquake loss estimation and loss disaggregation in buildings. Report No. 157. The John A. Blume Earthquake Engineering Center, Department of Civil and Environmental Engineering, Stanford University, Stanford, CA, USA, 2005.

[18] K.J. Elwood, J.P. Moehle. Axial capacity model for shear-damaged columns. *ACI Structural Journal*, **102**(4), 578-587, 2005a.

[19] K.J. Elwood, J.P. Moehle. Drift capacity of reinforced concrete columns with light transverse reinforcement. *Earthquake Spectra*, **21**(1), 71-89, 2005b.

[20] L. Zhu, K.J. Elwood, T. Haukaas. Classification and seismic safety evaluation of existing reinforced concrete columns. *Journal of Structural Engineering*, **133**(9), 1316-1330, 2007.

[21] W.M. Ghannoum. Re-evaluation of modeling parameters and acceptance criteria for non-ductile and splice-deficient concrete columns. *16th World Conference on Earthquake Engineering*, Santiago, Chile, January 9-13, 2017.

[22] W.M. Ghannoum, A.B. Matamoros. Nonlinear modeling parameters and acceptance criteria for concrete columns. *ACI Special Publication*, **297**, 1-24, 2014.

[23] S. Alath, S.K. Kunnath. Modelling inelastic shear deformations in RC beam–column joints. *10th Conference in Engineering Mechanics*, Boulder, Colorado, USA, May 21–24, 1995.

[24] M.T. De Risi, P. Ricci, G.M. Verderame. Modelling exterior unreinforced beam-column joints in seismic analysis of non-ductile RC frames. *Earthquake Engineering and Structural Dynamics*, **46**(6), 899-923, 2017.

[25] O.C. Celik, B.R. Ellingwood. Modeling beam-column joints in fragility assessment of gravity load designed reinforced concrete frames. *Journal of Earthquake Engineering*, **12**(3), 357-381, 2008.

[26] J.S. Jeon, L.N. Lowes, R. DesRoches, I. Brilakis. Fragility curves for non-ductile reinforced concrete frames that exhibit different component response mechanisms. *Engineering Structures*, **85**, 127-143, 2015.

[27] M.T. De Risi, G.M. Verderame. Experimental assessment and numerical modelling of exterior non-conforming beam-column joints with plain bars. *Engineering Structures*, **150**, 115-134, 2017.

[28] M.T. De Risi, P. Ricci, G.M. Verderame, G. Manfredi. Experimental assessment of unreinforced exterior beam-column joints with deformed bars. *Engineering Structures*, **112**, 215-232, 2016.

[29] C.P. Pantelides, J. Hansen, J. Nadauld, L.D. Reaveley. Assessment of reinforced concrete building exterior joints with substandard details. Pacific Earthquake Engineering Research Center, Report 2002/18, Berkeley, California, USA, 2002.

[30] C. Clyde, C.P. Pantelides, L.D. Reaveley. Performance-based evaluation of exterior reinforced concrete buildings joints for seismic excitation. Pacific Earthquake Engineering Research Center, Report 2000/05, Berkeley, California, USA, 2000.

[31] J.S. Jeon. Aftershock vulnerability assessment of damaged reinforced concrete buildings in California. PhD Dissertation. School of Civil and Environmental Engineering, School of Civil and Environmental Engineering at Georgia Institute of Technology, 2013.

[32] L.D. Decanini, G.E. Fantin. Modelos simplificados de la mampostería incluidas en porticos. Características de rigidez y resistencia lateral en estado límite. *Actas de las VI Jornadas Argentinas de Ingenieria Estructural*, Buenos Aires, Argentina, October 1–3, 1986. (in Spanish)

[33] L.D. Decanini, L. Liberatore, F. Mollaioli. Strength and stiffness reduction factors for infilled frames with openings. *Earthquake Engineering and Engineering Vibration*, **13**(3), 437– 454, 2014.

[34] N.M. Noh, L. Liberatore, F. Mollaioli, S. Tesfamariam. Modelling of masonry infilled RC frames subjected to cyclic loads: State of the art review and modelling with OpenSees. *Engineering Structures* **150**, 599–621, 2017.

[35] D. Cardone, G. Perrone. Developing fragility curves and loss functions for masonry infill walls, *Earthquakes and Structures*, **9**(1), 257–279, 2015.

[36] L. Liberatore, F. Noto, F. Mollaioli, P. Franchin. In-plane response of masonry infill walls: Comprehensive experimentally-based equivalent strut model for deterministic and probabilistic analysis. *Engineering Structures*, **167**, 533–548, 2018.

[37] K. Sassun, T.J. Sullivan, P. Morandi, D. Cardone. Characterising the in-plane seismic performance of infill masonry. *Bulletin of the New Zealand Society for Earthquake Engineering*, **49**(1), 98–115, 2016.

[38] A. Masi, A. Digrisolo, G. Santarsiero. Concrete strength variability in Italian buildings: analysis of a large database of core tests. *Applied mechanics and materials*, **597**, 283-290, 2014.

[39] M. Terrenzi, E. Spacone, G. Camata. Collapse limit state definition for seismic assessment of code‐conforming RC buildings. *International Journal of Advanced Structural Engineering*, **10**(3), 325–337, 2018.

[40] W.M. Hassan, J.P. Moehle. Quantification of residual axial capacity of beam-column joints in existing concrete buildings under seismic load reversals. *4th International conference on computational methods in structural dynamics and earthquake engineering – COMPDYN 2013*, Kos Island, Greece, June 12 – 14, 2013.

[41] M. Baradaran Shoraka, T.Y. Yang, K.J. Elwood. Seismic loss estimation of non-ductile reinforced concrete buildings. *Earthquake Engineering and Structural Dynamics*, **42**(2), 297-310, 2013.

[42] S. Sattar, A.B. Liel. Collapse indicators for existing nonductile concrete frame buildings with varying column and frame characteristics. *Engineering Structures*, **152**, 188-201, 2017.

[43] S. Hak, P. Morandi, G. Magenes, T.J. Sullivan. Damage control for clay masonry infills in the design of RC frame structures. *Journal of Earthquake Engineering*, **16**(sup1), 1-35, 2012.

[44] P. Ricci, M.T. De Risi, G.M. Verderame, G. Manfredi. Procedures for calibration of linear models for damage limitation in design of masonry-infilled RC frames. *Earthquake Engineering and Structural Dynamics*, **45**(8), 1315–1335, 2016.

[45] A. Masi, V. Manfredi, G. Cetraro. In-plane performance of RC infilled frames under seismic actions: Experimental versus code provision values. *16th International Brick and Block Masonry Conference*, Padova, Italy, June 26-30, 2016.

[46] M.T. De Risi, C. Del Gaudio, P. Ricci, G.M. Verderame. In-plane behaviour and damage assessment of masonry infills with hollow clay bricks in RC frames. *Engineering Structures*, **168**, 257–275, 2018.

[47] C. Del Gaudio, M.T. De Risi, P. Ricci, G.M. Verderame. Empirical drift-fragility functions and loss estimation for infills in reinforced concrete frames under seismic loading. *Bulletin of Earthquake Engineering*, **17**(3), 1285-1330, 2019.